Journal of The Electrochemical Society, **158** (3) D178-D186 (2011)
0013-4651/2011/158(3)/D178/9/$28.00 © The Electrochemical Society

Characterization and Purification of Commercial SPS and MPS by Ion Chromatography and Mass Spectrometry

Ryan G. Brennan,[a] Melissa M. Phillips,[a] Liang-Yueh Ou Yang,[b] and Thomas P. Moffat[b,*,z]

[a]*Analytical Chemistry Division, and* [b]*Metallurgy Division, Material Measurement Laboratory, National Institute of Standards and Technology, Gaithersburg, Maryland 20899-8551, USA*

SPS (bis-(3-sulfopropyl) disulfide) is an essential electrolyte additive used in the fabrication of copper interconnects by electrodeposition. In electroplating baths, the disulfide component of SPS may be cleaved to form the thiol analog, MPS (3-mercaptopropyl sulfonate), by either homogenous interactions with the Cu(I) reaction intermediate or by dissociative adsorption onto the copper surface. However, mechanistic studies into the role of these additives in copper electrodeposition are presently constrained by limited knowledge of the purity of commercially available SPS and MPS. This report details the use of ion chromatography (IC) and electrospray ionization mass spectrometry to characterize aqueous solutions of commercial SPS and MPS source materials. Sulfate (2.0%) and propane disulfonic acid (0.9%) (PDS) were determined to be the principal impurities in SPS (96.3% estimated purity, mass fraction). IC fractionation was used to purify and isolate SPS for surface and electroanalytical studies. Stability of SPS, MPS, and PDS in the presence of O_2 and Cu(II) was also examined. No degradation of SPS or PDS in aqueous solution was observed over a 3-month period. Solutions of MPS were metastable to O_2 saturation, but the addition of Cu(II) resulted in formation of SPS by dimerization as well as parasitic PDS generation.
 [DOI: 10.1149/1.3537819]

Manuscript submitted November 15, 2010; revised manuscript received December 20, 2010. Published January 21, 2011.

State-of-the-art Cu wiring for microelectronic circuitry is fabricated by electrochemical deposition.[1,2] The electroplating process requires the use of a specific combination of additives in an acidic Cu(II) plating bath to enable void-free filling of recessed surface features such as trenches and vias. Commercial additive packages comprised at least three species: Cl^-, an accelerator such as bis-(3-sulfopropyl) disulfide (SPS), and a polyether-based suppressor such as polyethylene glycol (PEG) or a related block or branched copolymer.[3,4] Chloride is a required coadsorbate for the formation of the inhibiting PEG layer as well as the subsequent formation of the SPS-derived accelerating surface phase. Feature filling involves a competition between SPS and the polyether for Cl^--saturated Cu surface sites.[2,3] As the local surface area decreases, such as within a filling trench, the more tightly bound SPS-derived adsorbates remain on the surface while the polyether suppressor is displaced into the electrolyte. This displacement results in an accelerated rate of Cu deposition on the SPS-enriched concave surface segments, leading to bottom–up superconformal filling. Several quantitative descriptions of feature filling based on the curvature enhanced accelerator coverage (CEAC) mechanism are available.[2-6] Nevertheless, much remains unknown about the physical and chemical nature of the SPS-derived accelerator surface phase.

A recent scanning tunneling microscope (STM) study of SPS adsorption on a Cl^- saturated Cu(100) surface revealed a plurality of lattice gas species diffusing on top of, or within, the Cl^- adlayer.[7] In addition to the dimer-like SPS species, smaller molecules suggestive of the related thiol monomer known as MPS (3-mercaptopropyl sulfonate) were also evident. MPS could be formed by a dissociative reductive adsorption of SPS dimers at defects within the Cl^- covered Cu surface. Alternatively, Cu(I), a well-established reaction intermediate in both the Cu deposition and dissolution reactions, may react homogenously with SPS to produce MPS that subsequently may adsorb to form thiolate species within the Cl^- adlayer. Such metal ion-mediated thiol/disulfide redox chemistry is widely known in synthetic organic chemistry and biology. In the case of electroplating, Cu(I) generation at Cu anodes has been a source of significant bath aging, causing difficulties both in printed circuit board fabrication[8] and more recently in Damascene wafer plating.[9] Subsequent use of proton-selective membranes to separate the anode and cathode compartments has significantly reduced Cu(I) generation, such that the only source of Cu(I) in the work piece compartment is that generated immediately adjacent to the electrode interface.[10-12] The concentration of Cu(I) is an exponential function of potential, with the prospect for homogenous Cu(I)/SPS chemistry being most significant during metal deposition at small overpotentials.[2] In a free standing electrolyte, MPS is thought to be unstable to oxidative dimerization by Cu(II) to form SPS and Cu(I), among other possiblities.[8,10,13] For plating cells open to the atmosphere, Cu(I) species are also constantly being scavenged by O_2 to regenerate Cu(II). Adding to the above complexity are results from recent voltammetric and STM experiments in our laboratory indicate that indicate the rate constant for MPS adsorption on a Cl^- saturated surface may exceed that of SPS by a factor of 100 or more. Such a significant difference opens the possibility that the low levels of MPS might dominate studies formally aimed at quantifying the kinetics of SPS adsorption. Unambiguous knowledge of the purity of the commercially available starting materials is required to rigorously evaluate the relative contributions of the respective disulfide and thiol species to the formation and function of the accelerator surface phase. Such knowledge will also support the development of a more quantitative understanding the Cu(I)/Cu(II) disulfide/thiol redox chemistry and its interaction with O_2.

Beyond the mechanistic concerns detailed above, industrial users have spent significant effort in development of tools for online measurements of the mass fractions and stability of SPS and related decomposition products that arise during electrolysis. Cyclic voltammetric stripping has been widely used for additive control, whereby the influence of the additives on the rate of metal deposition is monitored via integrated charge.[13,14] Some potential-dependent information is lost by integration; therefore, a more detailed analysis of the voltammetry or chronoamperometry represents an interesting opportunity for further refinement.[2,4] In a related fashion, the application of impedance methods is also being explored.[15] Similarly, a variety of other analytical methods (e.g., chromatography) have been developed for direct speciation of the additives and their breakdown products.[16-18] Online quantitative mass spectrometry has also been considered to track the accumulation of SPS and PEG breakdown products in practical plating baths.[12,19-22] These studies verified that SPS breakdown was oxidative with the most rapid deterioration being associated with reactions occurring at the anode. A variety of oxidation products were identified, but no account of the purity or speciation of the initial source materials was provided.

In order to develop a more detailed view of the structure, composition, and dynamics of the SPS/MPS derived accelerator surface phase, this work utilizes ion chromatography (IC) and mass spec-

* Electrochemical Society Fellow.
z E-mail: thomas.moffat@nist.gov

Table I. Selected ions used for characterization of electrolyte additives.

Compound (M)	Ion	*m/z*
SPS 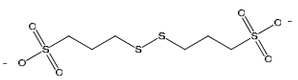	$[M-H]^-$	309
	$[M-2H]^{2-}$	154
	$[M-2H+Na]^-$	331
	unknown	186
MPS 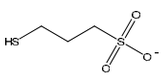	$[M-H]^-$	155
	$[2M-2H+Na]^-$	333
PDS 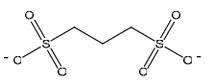	$[M-H]^-$	203
	$[M-2H]^{2-}$	101
	$[M-2H+Na]^-$	225

[a] pKa=10.84 for sulfhydryl based on known value for 2-mercaptopropionic acid.

trometry (MS) to characterize the source materials. A purification scheme for generation of higher-purity material based on IC fractionation was also implemented for subsequent surface and electroanalytical studies. Propane disulfonic acid (PDS), the reported end-stage oxidation product in SPS bath aging studies,[12,19-22] was also examined and found to be important for the correct IC speciation of the SPS source material. More specifically, when separation of the anions is performed in a potassium hydroxide (KOH) eluent, the sulfhydryl group of MPS^- is deprotonated, such that MPS^{2-} and PDS^{2-} exhibit a very similar transport behavior necessitating careful analysis. The influence of Cu(II) and O_2 on the stability of aqueous solutions of the source materials was also examined. The IC separations in combination with an MS assessment of the isotope distributions for MPS and SPS enabled a quantitative assessment of the conversion efficiency associated with Cu(II)/Cu(I) thiol/disulfide redox chemistry.

Experimental

Materials.— This investigation focused on two additive molecules, SPS and MPS, and a related compound, PDS, as shown in Table I. All sample preparations were performed using water with a resistivity of 18.2 M Ω cm. The SPS, disodium salt (96%) was obtained from Raschig (Ludwigshafen, Germany) and PDS, disodium salt (98%) was obtained from Avocado Research Chemicals, Ltd. (Heysham, Lancashire, United Kingdom).[c] Two different sources of MPS were investigated, from Sigma-Aldrich (St. Louis, MO) (90%) and Raschig (94.9% approximately). No measureable differences were observed between the two sources of MPS. NIST Standard Reference Material (SRM) 3181 Sulfate Anion Standard Solution was also examined for impurity identification and quantification. Analytical reagent-grade cupric sulfate used in the stability studies was obtained from Mallinckrodt (Paris, KY).

Sample preparation.— Compound purity was evaluated initially by gravimetric preparation of solutions of approximately 200 mmol L^{-1} SPS, 10 mmol L^{-1} MPS, and 5 mmol L^{-1} PDS in ultrapure water. For determination of the IC linear range, serial dilutions were prepared from the aqueous stock solutions to give concentrations in the range of 0.3–12.0 mmol L^{-1}. The stability of the source materials in the presence of various concentrations of $CuSO_4$ with and without O_2 saturation was also examined. After exposure to $CuSO_4$, samples were passed through a solid-phase strong cation exchange (SCX) cartridge (500 mg, Alltech Associates, Inc., Deerfield, IL) to remove the high concentration of Cu(II) prior to IC or MS analysis. If not removed, the Cu(II) can damage the IC analytical column, IC suppressor unit, and MS quadrupole.

[c] Identification of commercial products in this paper was done to specify the experimental procedure. In no case does this imply endorsement or recommendation by the National Institute of Standards and Technology.

Table II. IC operating conditions.

Guard column	Ion-Pac AG11-HC, 4 × 50 mm
Separation column	Ion-Pac AS11-HC, 4 × 250 mm
Suppressor	ASRS-300 (4 mm)
Suppression current	100 mA
Injection loop volume	25.0 μL
Eluent generator cartridge	EG40 (4 M KOH)
Online eluent generation	Step gradient
Eluent concentration (KOH)	0–20 min: 15 mmol L^{-1} 20–25 min: 15–50 mmol L^{-1} 25–30 min: 50 mmol L^{-1} 30–40 min: 50–15 mmol L^{-1}
GP50 gradient pump	1.00 mL min^{-1}
LC30 chromatography oven	30°C
Pressure	13,800 kPa
PDS peak retention time	10.2 min (average)
MPS peak retention time	10.5 min (average)
SPS peak retention time	32.4 min (average)
Quantification	Peak area
Data collection rate	5.0 Hz

IC.— Chromatography was performed with the Dionex DX-500 IC system (Dionex Corporation, Sunnyvale, CA) consisting of a GP50 gradient pump, an LC30 chromatography oven, an EG40 eluent generator, an AS40 autosampler, and a CD20 conductivity detector with suppressor (ASRS-300). The gradient pump delivered deionized (DI) water (18 M Ω cm) to the eluent generator, which converted the DI water to a high-purity KOH eluent by an applied dc current. As specified in Table II, a step gradient of KOH was used in combination with a guard column and analytical column to resolve components in a 25-μL sample injection. After separation, the column effluent was passed through the suppressor unit to neutralize the eluent, reduce the background conductance, remove the counterions from the sample, and convert analyte ions to a single highly conductive form. In combination, these factors lead to enhanced sensitivity and lower detection limits. The column oven was set to 30°C to prevent baseline drift due to temperature disruption. The Chromeleon Client software (version 6.70, Build 1820) provided control of the Dionex DX-500 IC system and all components listed above, allowing automation of the chromatographic analyses, in addition to providing a data analysis tool for quantitative results.

To collect IC peak fractions for analysis by MS, the ASRS-300 was operated in external water mode. The output from the conductivity cell was disconnected from the suppressor unit and replaced with tubing of known length and inner diameter for accurate calculation of collection time for the analyte peak of interest. To replenish the suppressor unit, a constant flow of DI water (18 M Ω cm) was delivered to the suppressor from a Teflon bottle pressurized with nitrogen gas. With this setup, the analyte peak of interest was monitored by the conductivity detector and analyzed post-collection by MS. The same method was used to generate high-purity samples for further electroanalytical and surface analytical studies.

Electrospray ionization mass spectrometry (ESI-MS).— A liquid chromatograph equipped with a single quadrupole mass spectrometer was utilized in flow-injection mode for analysis of MPS, SPS, and PDS samples. MS-grade water was used for sample introduction

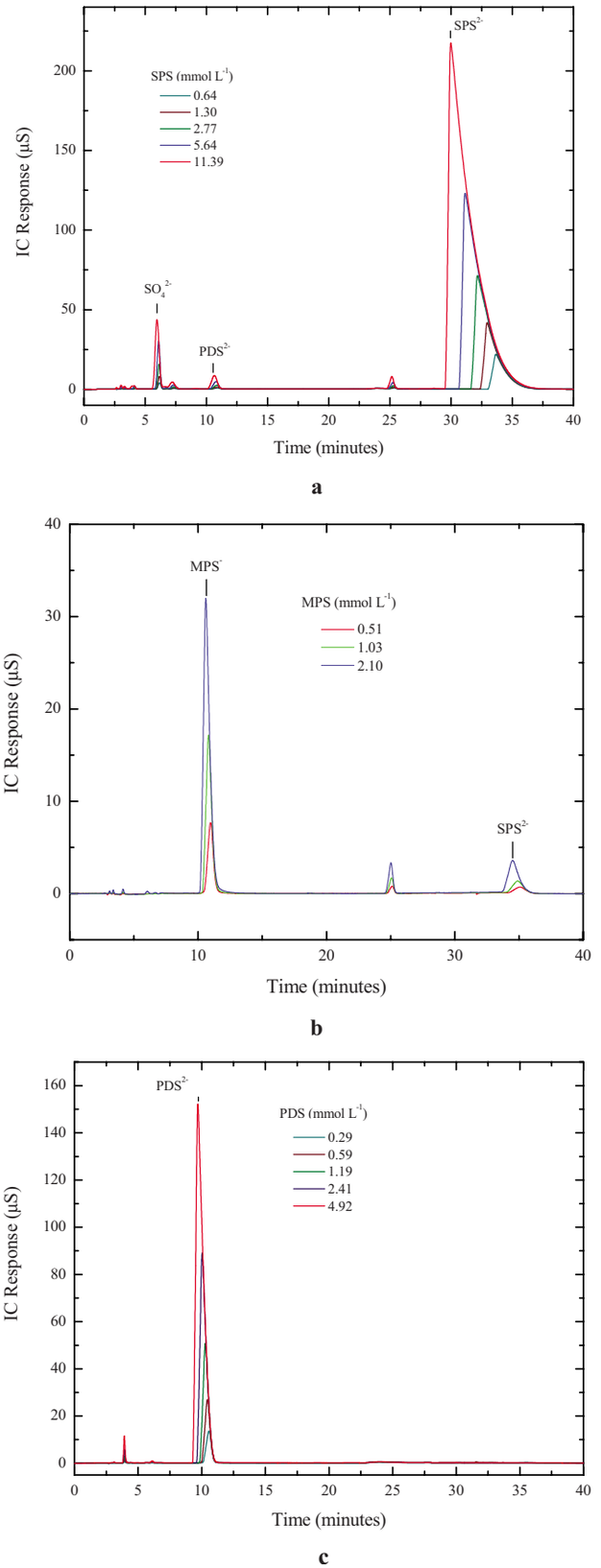

Figure 1. (Color online) Ion chromatograms of aqueous solutions of (a) SPS, (b) MPS, and (c) PDS source materials.

at a flow rate of 0.5 mL min^{-1}. For analysis of stock solutions, a 1-μL injection volume was used. For analysis of IC fractions, a 20-μL injection volume was used. The MS was operated in negative ion mode with atmospheric pressure electrospray ionization (API-ESI). The ESI source was operated with a capillary voltage of 2000 V, a fragmenter voltage of 90 V, a drying gas temperature of 350°C and flow rate of 12 L min^{-1}, and a nebulizer pressure of 379 kPa. The MS was utilized in both scanning and selected ion monitoring (SIM) modes. Common ions observed for MPS, SPS, and PDS are summarized in Table I.

Results and Discussion

Purity of source materials.— This work utilized IC and MS to characterize the SPS, MPS, and PDS source materials for a more detailed view of the structure, composition, and dynamics of the SPS/MPS derived accelerator surface phase. Chromatograms for increasing concentrations of aqueous solutions of the SPS, MPS, and PDS source materials were used to establish calibration curves and are shown in Fig. 1. The calibration data derived from these chromatograms are listed in Table III, following correction for the estimated impurity content in the source materials, summarized in Table IV. The concentrations and uncertainties of the known impurities were determined from the average of the impurity calculated from the calibration curves and the impurity calculated from the relative IC peak area. The unidentified impurities were determined solely from the relative IC peak area. Percent purities determined by using IC peak area assume the conductance of the individual species is independent of concentration, and the conductance was taken to be that of the major component. Corresponding MS data for representative samples are shown in Fig. 2, with assignments of the major ions associated with each compound already summarized in Table I.

For SPS, the dominant anionic species was SPS^{2-} (96.2%), which eluted between 30 and 35 min (Fig. 1a). The integrated peak area increased and the elution time of the peak front decreased monotonically with the increasing SPS^{2-} concentration. The peak shape became increasingly asymmetric with increasing concentration, indicating increasing saturation of the chromatographic surface sites with the increasing SPS concentration. The elution time of the peak tail was reproducible as a function of concentration, reflecting the specific desorption kinetics of SPS^{2-} with the chromatographic gradient conditions. Data from fractionation of the IC chromatogram corresponding to the peak at 30 min (Fig. 2a) confirmed the identity of this peak as SPS. The second largest peak observed in the chromatogram of the SPS source material eluted between 6 and 7 min. This peak was attributed to SO_4^{2-} (2.0%) based on favorable comparison with the SRM 3181 Sulfate Anion Standard Solution as well as MS analysis of the fractionated peak. A third peak evident near 11 min was ascribed to PDS^{2-} (0.9%), as detailed below. Expansion of the ordinate (not shown) revealed nine additional minor peaks, two of which were discounted as artifacts based on control experiments. MS analysis of the corresponding fractionated samples proved inconclusive. The unidentifiable peaks contributed to a total of less than 1.0% impurities. Linear regression of the calibration plots for SPS based on peak area and peak height are summarized in Table III. Three replicates of five concentrations were measured, providing a relative standard deviation (RSD) of 0.3 and 0.4% for peak height and peak area, respectively. The calibration plot based on peak area was linear over the evaluated range, with a correlation coefficient of 1.0000.

A series of chromatograms for MPS are shown in Fig. 1b, with the dominant peak eluting near 11 min. During the IC separation, the alkaline mobile phase caused deprotonation of the sulfhydryl head group of MPS, leaving the analyte present as the doubly charged anion, MPS^{2-}. As with SPS^{2-}, the elution time of the peak tail for MPS^{2-} was reproducible for the different concentrations, reflecting the specific desorption kinetics of MPS^{2-} with the chromatographic gradient conditions. Data from fractionation of the IC eluent corresponding to the peak at 11 min (Fig. 2b) confirmed the

Table III. IC calibration results for aqueous solutions of SPS, MPS, PDS, and SO_4^{2-}. For each calibration curve, five concentrations ($n = 5$) were measured in replicates of three, providing mean retention times and a relative standard deviation (%RSD) for retention time, peak height, and peak area. In the line equations, x, is equal to moles per liter, for SPS, MPS, and PDS; for SO_4^{2-} x is equal to μg g^{-1}.

	Retention Time (min)		Peak Area (μS min)			Peak Height (μS)		
Compound	Mean	%RSD	%RSD	Equation	R^2 [c]	%RSD	Equation	R^2 [c]
SPS[a]	32.4	3.4	0.4	y = 20463x − 1.115	1.0000	0.3	y = 10767x + 9.539	0.9933
MPS[a]	10.5	3.7	3.2	y = 10386x − 1.751	0.9993	3.0	y = 11799x + 5.746	0.9943
PDS[a]	10.2	3.1	0.9	y = 21836x − 0.125	1.0000	0.6	y = 40358x + 2.236	0.9986
SO_4^{2-} [b]	6.7	0.2	0.7	y = 0.2348x + 1.269	0.9954	0.4	y = 0.8938x + 4.981	0.9954

[a] Data corrected for estimated purity of source materials.
[b] n = 3.
[c] R^2 represents the square of the correlation coefficient.

identity of this peak as MPS (87.2%). The second largest peak in the chromatogram for the MPS source material eluted at 35 min (7.0%). This peak was identified as SPS^{2-} based on the elution profile of the peak tail, which was consistent with that for the SPS source material, shown in Fig. 3a. A third prominent peak in the IC of the MPS source material eluted at 25 min (5.3%). A similar peak was also present at 25 min in the SPS chromatogram (0.4% SPS), but MS analysis of the fractionated peak was inconclusive. A broad background peak present in both the MPS and SPS IC chromatograms was also present in the blank injections and can be attributed to an artifact of the gradient elution procedure. The artifact was removed from the sample chromatograms by blank subtraction. Expansion of the chromatogram ordinate (not shown) revealed approximately ten additional minor peaks, which were not considered further ($< 1.0\%$). Linear regression of the calibration plots for MPS based on peak area and peak height are summarized in Table III. Three replicates of five concentrations were measured, providing a RSD of 3.0 and 3.2% for peak height and peak area, respectively. The calibration plot based on peak area was linear over the evaluated range, with a correlation coefficient of 0.9993.

The estimated purity of the PDS source material (98.5%) was higher than that of SPS or MPS. The dominant chromatographic peak at 10 min in Fig. 1c corresponded to PDS^{2-} as confirmed by MS (Fig. 2c). As with the other species of interest, the PDS^{2-} peak was asymmetric with a consistent elution time for the peak tail, reflecting the specific column desorption kinetics of PDS^{2-} with the gradient elution program. Expansion of the ordinate revealed five additional minor peaks that were not identified by IC or MS and, therefore, not considered further ($< 2.0\%$). Linear regression of the calibration plots for PDS based on peak area and peak height are summarized in Table III. Three replicates of five concentrations were measured, providing an RSD of 0.6 and 0.9% for peak height and peak area, respectively. The calibration plot based upon peak area was linear over the evaluated range, with a correlation coefficient of 1.0000.

Chromatograms for 5.52 mmol L^{-1} SPS, 1.53 mmol L^{-1} MPS, and 2.42 mmol L^{-1} PDS are presented in Fig. 3a. The elution times for PDS^{2-} and MPS^{2-} were very similar as a consequence of the similar molecular size and charge distribution of PDS^{2-} and MPS^{2-} during the separation. This similarity may account for some of the ambiguities and uncertainties in SPS/MPS speciation in previous chromatographic studies. Despite their similar elution times, the conductivity of MPS solution was substantially lower than that for PDS. Because detection occurs after IC separation and ion suppression, the *p*H of the eluent decreased, causing MPS^{2-} to be protonated to MPS^-, thus carrying half the charge of PDS^{2-}. This difference is reflected in the slope of the peak area calibration curves, with the slope for the PDS^{2-} curve being approximately twice that for the MPS curve.

The difference in IC column desorption kinetics of PDS^{2-} and MPS^{2-} was particularly helpful for impurity speciation of the SPS source material. For example, the doublet peak could be clearly resolved for a controlled mixture of MPS and PDS (Fig. 3c). Furthermore, the specific desorption kinetics of the respective species enabled the peak tail shape to be used analytically. As shown in Fig. 3a and 3b, comparison of the peak eluting between 10 and 11 min in the SPS chromatogram to that for MPS^{2-} and PDS^{2-} chromatograms indicated that the impurity in the SPS material was PDS^{2-}. The identity of the impurity was confirmed as PDS by offline MS measurements of a small quantity of the IC peak based on an observed mass-to-charge ratio (m/z) of 202.

Stability of source materials.— Significant aging effects have been reported in practical additive-based electroplating, particularly when a Cu anode was used in an unseparated electrochemical cell. A large number of studies have reported degradation effects associated with interactions between Cu(II)/Cu(I) and SPS^{2-}/MPS^- in these types of cells.[8-22] At the same time, interactions with atmospheric O_2 and the reduction intermediate H_2O_2 may also have a direct or indirect role in thiol/disulfide chemistry.[8,23] To investigate these inter-

Table IV. Estimated purity analysis results for commercial sources of SPS, MPS, and PDS by IC.[a]

		Mass Fraction (%)				
Compound	Source	SPS	MPS	PDS	SO_4	Other[b]
SPS	Raschig	96.4 ± 1.1		0.9 ± 0.1	2.0 ± 1.3	0.8 ± 0.06
MPS	Raschig	7.0 ± 0.7	87.2 ± 0.1			5.8 ± 0.04
PDS	ARC Ltd.			98.5 ± 0.04		1.5 ± 0.005

[a] Combined average and standard deviation of the purity assessment using peak area calibration curves from Table III and relative peak area assuming uniform conductance for all peaks, n = 3 (replicate injections) based upon a 95% confidence interval.
[b] Not able to identify species by IC or MS, all unidentifiable species are summed together assuming uniform conductance for all peaks. Uncertainty calculated from sum of squares of the standard deviation for n = 3 (replicate injections).

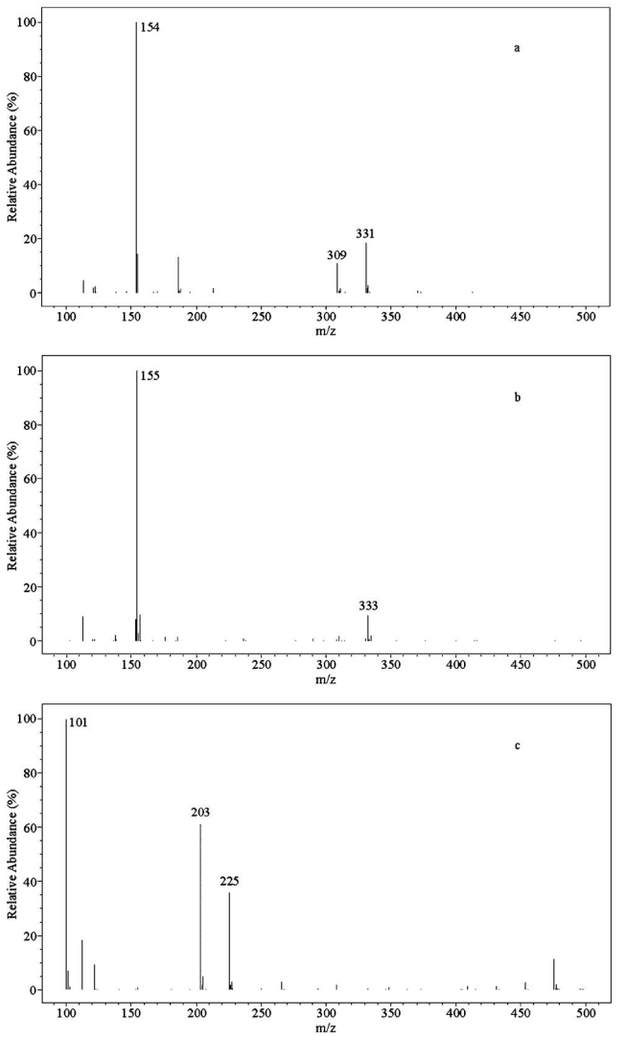

Figure 2. Mass spectra for aqueous solutions of (a) SPS, (b) MPS, and (c) PDS.

actions in more detail, the stability of the neat solutions in the presence of O_2 and Cu(II) were examined. Solutions of SPS^{2-} (5.52 mmol L^{-1}), PDS^{2-} (2.42 mmol L^{-1}), and MPS^{-} (1.53 mmol L^{-1}) were exposed to three treatments: (1) Ar-deaerated water, (2) O_2-saturated water, and (3) O_2-saturated solution containing 10 μmol L^{-1} $CuSO_4$. The samples were examined by IC. Additional studies in more concentrated $CuSO_4$ solutions (i.e., 2–5 mmol L^{-1}) were also performed.

Extended aging of SPS^{2-} and PDS^{2-} in O_2-saturated solutions in the presence and absence of Cu(II) revealed no change in the IC response beyond an increase in $SO4^{2-}$ concentration from the addition of Cu(II). Similarly, MS analysis revealed inconsequential changes (Fig. 2 and 4), detailed below. The inert behavior of SPS under these conditions was consistent with prior electrolyte aging studies, indicating that in the absence of Cu(I) species, no significant alteration of SPS^{2-} occurs.[8,10]

The same experiments were performed with the MPS source material. Sparging with O_2 had no measurable effect on MPS^{-} speciation, as the IC response was unaltered for up to 2 weeks after solution preparation. In contrast, the addition of 10 μmol L^{-1} Cu(II) resulted in a decrease in MPS peak intensity by IC. As shown in Fig. 5a and 5b, the addition of 2.14 mmol L^{-1} $CuSO_4$ to a 1.53 mmol L^{-1} MPS solution resulted in complete disappearance of

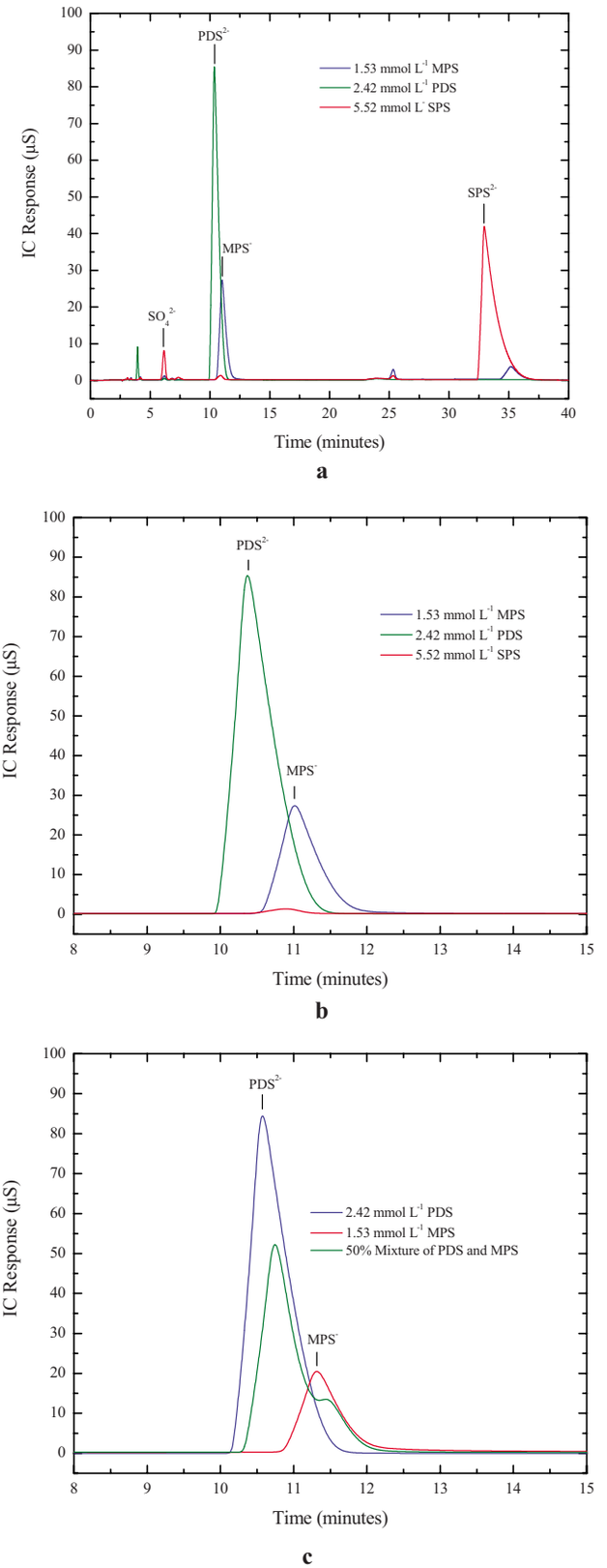

Figure 3. (Color online) (a) Ion chromatograms for similar concentration of SPS, MPS, and PDS. The SPS^{2-} impurities in MPS are evident along with the similar elution time of MPS^{2-} and PDS^{2-}. (b) Close examination of the peak tail is helpful for MPS^{2-} and PDS^{2-} speciation. (c) In a physical mixture of MPS^{2-} and PDS^{2-}, the chromatographic peaks can be deconvoluted.

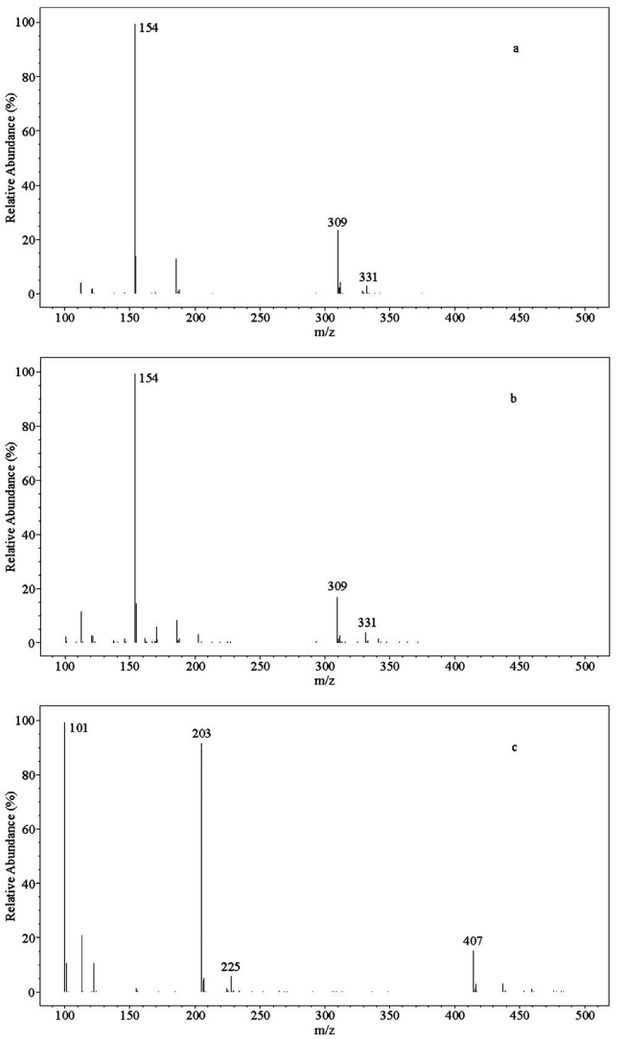

Figure 4. Mass spectra for aqueous solutions of (a) SPS, (b) MPS, and (c) PDS following exposure to Cu(II).

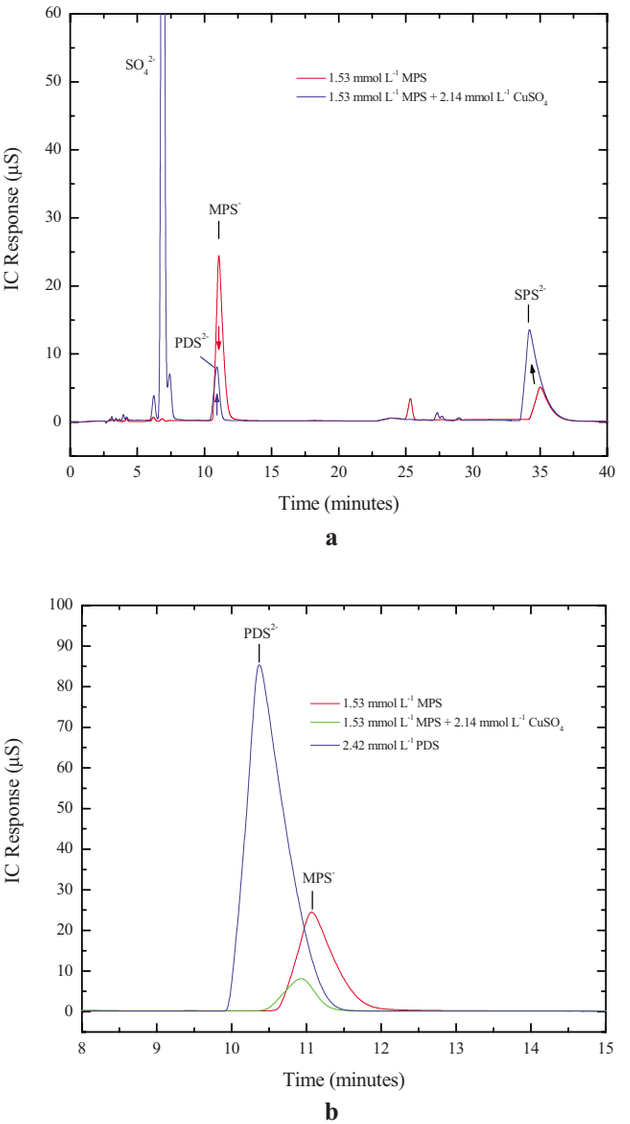

Figure 5. (Color online) (a) Ion chromatograms reveal the Cu(II)-induced competitive oxidative dimerization of MPS^{2-} to SPS^{2-} and oxidation to PDS^{2-}. (b) A higher resolution version depicts the conversion of 0.18 mmol L^{-1} MPS^{2-} to 0.18 mmol L^{-1} PDS^{2-}, approximately 12% w/w MPS.

the MPS^- peak. This disappearance was accompanied by the appearance of a smaller peak at a slightly earlier elution time consistent with the formation of PDS^{2-} and an increase in the intensity of the peak at 35 min corresponding to SPS^{2-}. The peak position and tail shape associated with analysis of stable PDS^{2-} and SPS^{2-} solutions, as well as MS analysis, confirmed these as the identities of newly formed species. Taken together, these results indicated that exposure to Cu(II) leads to the oxidative conversion of MPS^- to a combination of SPS^{2-} and PDS^{2-}, as well as other minor impurities. Most Cu(II)-free MPS preparations proved time stable although some decay was evident for a subset of samples that is believed to be due to spurious contamination, most likely Cu(II), or perhaps some effect of light exposure. Comparison of MPS solutions before and after Cu(II) additions allows a quantitative assessment of the partitioning between the different breakdown products. Using the calibration information given in Table III, the initial solution contained 1.53 mmol L^{-1} of MPS^- and 0.32 mmol L^{-1} SPS^{2-}. Within 24 h of exposure to Cu(II), the final SPS^{2-} and PDS^{2-} concentrations were 0.87 and 0.18 mmol L^{-1}, respectively. The increase in concentration of SPS^{2-} by 0.55 mmol L^{-1} corresponded to the dimerization of 1.11 mmol L^{-1} MPS^-, while the parallel PDS^{2-} reaction channel resulted in the oxidation of an additional 0.18 mmol L^{-1} MPS^-. Approximately 0.24 mmol L^{-1} or 15% of the original MPS^- remained distributed between other species such as sulfones, consistent with the MS results discussed below.

Isotopic abundance and MS speciation.— As described in Table I, the *m*/*z* of MPS^- and SPS^{2-} differ by a single mass unit. However, the natural isotopic abundances of the atomic components of SPS, MPS, and PDS allow distinctions between MS data for these compounds with their very similar *m*/*z,* even on a low-resolution instrument such as a single quadrupole. The distributions of the major natural isotopes of sulfur (^{32}S = 95.02% and ^{34}S = 4.21%) and carbon (^{12}C = 98.9% and ^{13}C = 1.01%) are the major contributors to these unique isotope distributions.

Reference mass spectra for SPS, MPS, and PDS acquired for the stock solutions prior to IC separation are shown in Fig. 2, and the assignments for the major ions are summarized in Table I. The observed isotope distributions for SPS^{2-}, MPS^-, and PDS^{2-} species in the stock solutions, as well as ratios predicted by natural isotopic

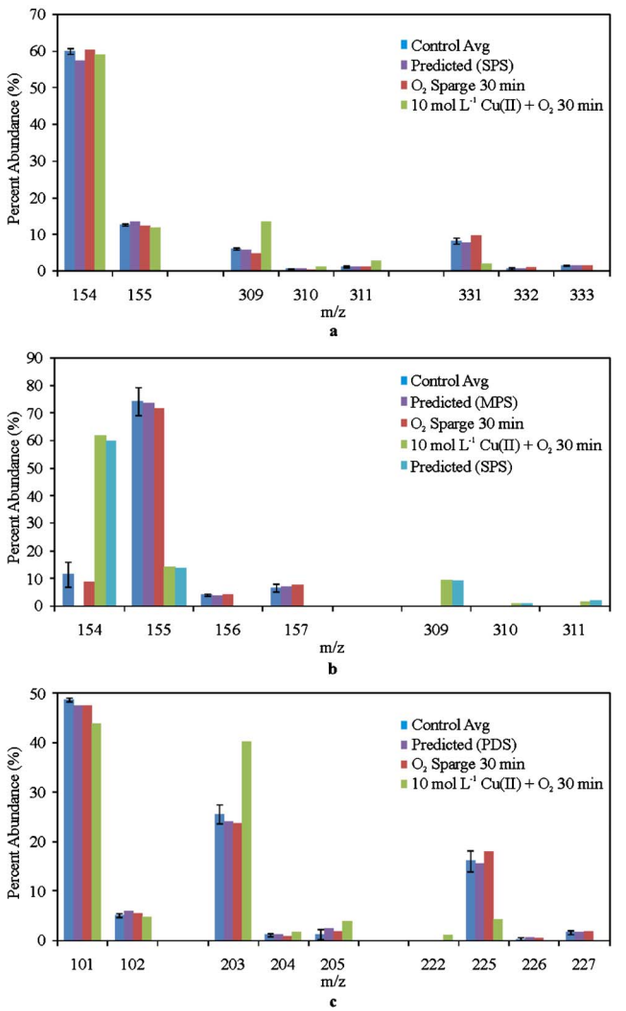

Figure 6. (Color online) Comparison of observed and predicted isotope ratios for (a) SPS, (b) MPS, and (c) PDS before and after various oxidative treatments.

distributions, are summarized in Fig. 6. Excellent agreement was found for the predicted and observed isotope ratios for solutions of SPS^{2-} and PDS^{2-}. The observed isotope ratios remained consistent with predicted ratios after extended exposure to O_2 and/or Cu(II). The observed signals for sodium adducts of SPS^{2-} and PDS^{2-} were reduced following the cation exchange cleanup used with the Cu(II) solution because the procedure removed both Cu(II) and Na^+ from the sample solutions, resulting in a higher fraction of protonated ions. Close inspection of the SPS material (Fig. 2a) revealed an additional species with m/z 186 and a relative abundance of 10%. Relative to SPS^{2-} the m/z corresponds to a mass increment corresponding to either two more S, or four more O atoms, or some combination thereof, suggestive of either a more extended sulfide or perhaps sulfone chemistry. The same m/z was evident in the IC fractions of the SPS^{2-} peak, implying that this MS peak was an unidentified fragmentation product of SPS^2 or perhaps an additional component that elutes at the same time as SPS^{2-}. The latter might favor the sulfone versus tetrasulfide chemistry.

Examination of the isotope ratios for an aqueous solution of the MPS source materials confirmed the majority species is MPS^-. An additional MS peak was evident at m/z 154, consistent with the presence of SPS^{2-} as an impurity. Qualitatively, the relative abundance of m/z 154 was about 10% the abundance of MPS^-, in excellent agreement with IC analysis. The isotope distribution in the MPS sample was not significantly altered by O_2 saturation. However, the addition of Cu(II) resulted in conversion of most of the MPS^- to SPS^{2-}. Close inspection of the MS data shown in Fig. 4 also revealed peaks at m/z 101, 170, 186, and 202 with monotonically increasing yield that did not exceed 20% abundance, relative to the SPS^{2-} peak at m/z 154. The peaks at m/z 101 and 202 correspond to PDS^{2-}, and the relative abundances were consistent with those determined by IC, with total PDS^{2-} production less than 10% relative to dimerization to SPS^{2-}. The peak at m/z 186 was attributed to an unidentified fragmentation product of SPS^{2-} as detailed in the previous paragraph. The peak at m/z 170 may correspond to a sulfone version of SPS^{2-} that has been reported by others.[12,20-22]

Recent studies of the oxygen reduction reaction on Cu suggest that oxidation of Cu(I) to Cu(II) might be associated with H_2O_2 generation.[23] Thus, in addition to cleaving the disulfide bond, Cu(I) interaction with O_2 may play a critical role in the partitioning between MPS^- dimerization to SPS^{2-} or to SPS^{2-}-sulfone to disulfone that may result in PDS^{2-} generation. Alternatively, PDS^{2-} formation may arise from direct oxidation of the thiol or Cu(I)-thiolate species. To probe this question further, a kinetic study as a function of the O_2 concentration might be helpful.

IC identified two oxidative pathways for Cu(II) reaction with MPS^-. For the conditions examined, the dominant reaction was dimerization of MPS^- to SPS^{2-}, while simultaneously a small fraction of MPS^- was converted to PDS^{2-}. Analysis by MS suggests the presence of at least one other species, most likely a sulfone (m/z 170), which was not present in the SPS^{2-} source material. Importantly, based on the insignificant adsorption of PDS^{2-} on the Cu surface, the sulfone group may be unlikely to affect adsorption of the low oxidation state disulfide (SPS^{2-}) or thiol (MPS^-) species and thus unlikely to impact the electrodeposition process.

SPS-Cl co-adsorption using purified SPS.— Recently, the accelerator surface phase responsible for superconformal film growth has been identified as an SPS-derived lattice gas supported on a Cl^- saturated surface.[7] The STM study revealed the development of a plurality of different species with an increased immersion time. Impurities associated with the SPS source material were identified as one potential source of this surface diversity. The present work indicates that the SPS source material is essentially free of MPS^-, with SO_4^{2-} and PDS^{2-} being the most significant impurities (Table IV). Furthermore, recent work has demonstrated that addition of PDS^{2-} to a Damascene plating bath up to 100 mmol L^{-1} had no significant effect on the Cu deposition rate.[7] Instead, the Cu growth rate was controlled by the competition between the SPS accelerator and inhibiting polyether additives. Accordingly, the conclusion that the PDS^{2-} impurity in SPS is of no practical consequence implies that the MPS-free source material may be suitable for analytical studies. Nevertheless some uncertainty remains as to the possible influence of the remaining 0.8% unidentified impurities and the unclear nature of the 186 m/z ratio species identified by MS.

To examine this issue more closely, in situ STM was used to image the SPS-derived adsorbate species formed from the commercial source materials in comparison to those formed from a purified sample. The SPS source material was purified by fractionation of a 43.32 mmol L^{-1} SPS solution and collection of the volume eluted between 27 and 35 min. The IC chromatograms for the source and purified materials are shown in Fig. 7. A control sample of water was run to establish that an asymmetric peak between 23 and 27 min was an artifact of the IC experiment; the chromatogram shown in Fig. 7 is blank corrected. Other than possible carryover of a small anionic species evident before 5 min in the chromatogram, the purified material exhibited only one peak at 33 min corresponding to SPS^{2-}.

An electropolished Cu(100) surface was immersed in a solution of 0.1 mol L^{-1} $HClO_4$ containing 1 mmol L^{-1} HCl at a potential close to −0.15 V versus Ag/AgCl. The c(2 × 2) Cl^- adlayer, where

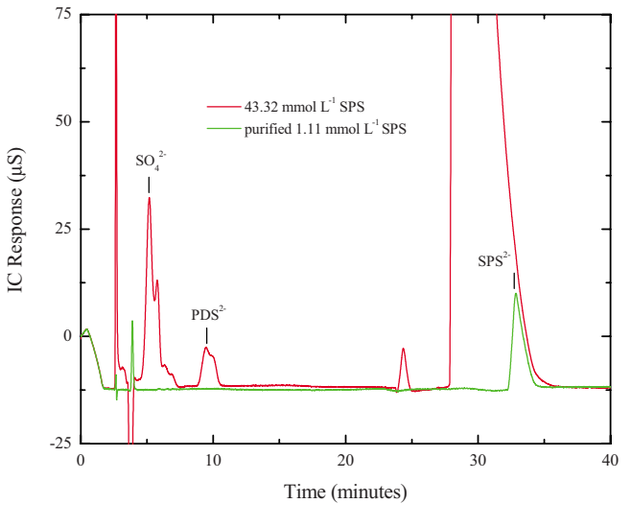

Figure 7. (Color online) Ion chromatograms (blank corrected) for a purified SPS^{2-} solution, obtained by collecting the 35 min peak fraction from the 43.32 mmol L^{-1} solution of the SPS source material.

Cl^- occupies every second fourfold hollow site on the primitive square lattice, immediately formed as detailed elsewhere.[7] Subsequently, an aliquot of either the unpurified SPS source material or purified SPS was added to give a concentration of 50 μmol L^{-1}, and the surface was continually imaged by STM, as described previously.[7] Representative STM images from both experiments are shown in Fig. 8. The square electron density pattern corresponds to c(2 × 2) Cl^- adlayer with a nearest neighbor spacing of 0.36 nm. A dilute coverage of the larger SPS-derived adsorbates was evident on the surface by their distinctive shape, size, and bright contrast. At least two different species were evident based on the arrangement of the electron density as well as their differing mobility as revealed by continuous monitoring. The similarity of the images obtained using the source and purified SPS materials suggested that source impurities were not responsible for the plurality of adsorbate states observed. Rather, the differences must be associated with distinct binding states of the SPS^{2-} precursor. Further studies of the structure and dynamics of SPS^{2-} adsorption are underway.

Conclusions

IC combined with ESI-MS revealed that the dominant impurities of commercial SPS are PDS^{2-} and SO_4^{2-}. Neither of these impurity species exerts a significant effect on Damascene Cu plating kinetics, and thus the source materials may be deemed acceptable in this context. Purified SPS may be easily obtained by IC fractionation, but preliminary in situ STM experiments of the SPS accelerator surface phase indicates that the plurality of adsorbate states were not related to impurities in the SPS source materials. More likely, the plurality arises from a variety of binding states derived from the adsorption process.

Commercial MPS was found to contain approximately 7.0% SPS as the major impurity. In the presence of Cu(II) and O_2, MPS was observed to be dimerized to SPS^{2-}. In addition, a small fraction of the MPS was oxidized to PDS^{2-} (12%). Whether the partitioning between these two reactions can be controlled by varying the relative concentration of the reactants [MPS^-, O_2 or Cu(II)] or the acidity remains to be determined. In unseparated Cu plating baths, Cu(I) generated at the anode leads to MPS formation by reduction of the available SPS. Cu(II) reacts with MPS to reform SPS by dimerization. In parallel with this reaction, some of the MPS is converted to PDS^{2-}. Previous analysis of plating baths shows this to be a significant degradation path for SPS chemistry used in Damascene plating.

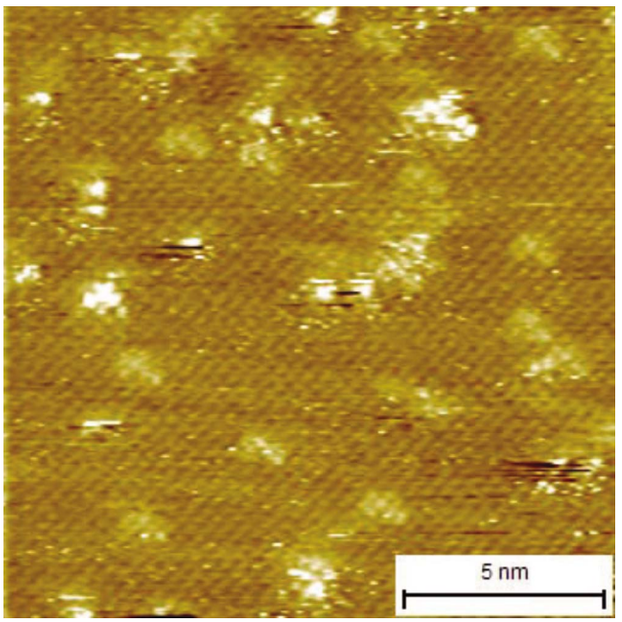

a

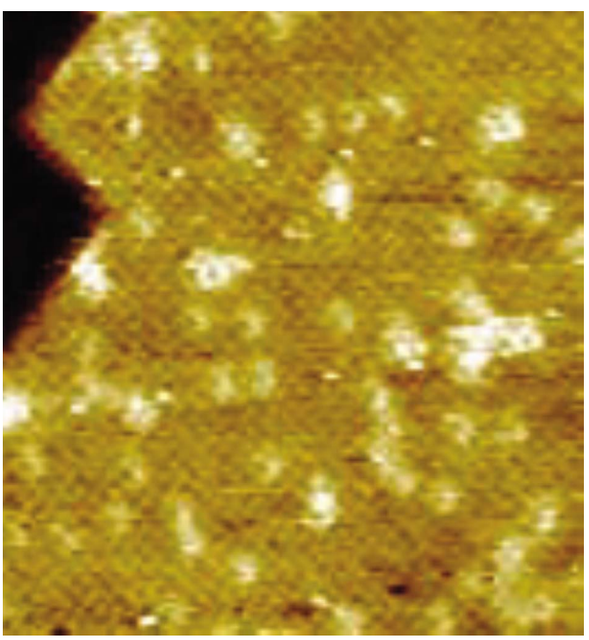

b

Figure 8. (Color online) In situ STM images of SPS-derived adsorbates on a Cl^- c(2 × 2) saturated Cu(100) surface. The respective experiments were performed using 50 μmol/L of either (a) the SPS source material or (b) the SPS^{2-} purified by IC. The experiments show that the multiplicity of SPS-derived adsorbates is a consequence of different binding states rather than an impurity effect.

The degradation process is greatly diminished if the anode is isolated from the working cell by a cation specific membrane as previously demonstrated.

National Institute of Standards and Technology assisted in meeting the publication costs of this article.

References

1. P. A. Andricacos, C. Uzoh, J. O. Dukovic, J. Horkans, and H. Deligianni, *IBM J. Res. Dev.*, **42**, 567 (1998).
2. T. P. Moffat, D. Wheeler, M. D. Edelstein, and D. Josell, *IBM J. Res. Dev.*, **49**, 19 (2005).
3. T. P. Moffat, D. Wheeler, and D. Josell, in *Advances in Electrochemical Science and Engineering*, Vol. 10, R. C. Alkire, D. M. Kolb, J. Lipkowski, and P. N. Ross, Editors, Wiley-VCH, Weinheim (2008).
4. J. W. Gallaway, M. J. Willey, and A. C. West, *J. Electrochem. Soc.*, **156**, D146 (2009).
5. A. Pohjoranta and R. Tenno, *J. Electrochem. Soc.*, **154**, D502 (2007); A. Pohjoranta and R. Tenno, *J. Electrochem. Soc.*, **155**, D383 (2008).
6. R. Akolkar and U. Landau, *J. Electrochem. Soc.*, **156**, D351 (2009).
7. T. P. Moffat and L.-Y. Ou-Yang, *J. Electrochem. Soc.*, **157**, D228 (2010).
8. J. P. Healey, D. Pletcher, and M. Goodenough, *J. Electroanal. Chem.*, **338**, 167 (1992).
9. J. Horkans and J. O. Dukovic, in *Electrochemical Processing in ULSI Fabrication III*, P. C. Andricacos, J. L. Stickney, P. C. Searson, C. Reidsema-Simpson, and G. M. Oleszek, Editors, PV 2000-8, p. 103, The Electrochemical Society Proceedings Series, Pennington, NJ (2002).
10. T. P. Moffat, B. Baker, D. Wheeler, and D. Josell, *Electrochem. Solid-State Lett.*, **6**, C59 (2003).
11. C. L. Beaudry and J. O. Dukovic, *Electrochem. Soc. Interface*, **13**(4), 40 (2004).
12. M. J. West, M. R. Anderson, Q. Wang, T. H. Bailey, A. Rosenfeld, Z.-W. Sun, and K. P. Ta, in *Electrochemical Processes in ULSI and MEMS*, H. Deligianni, T. P. Moffat, S. T. Mayer, and G. R. Stafford, Editors, PV 2004-17, p. 41, The Electrochemical Society Proceedings Series, Pennington, NJ (2005).
13. M. Pavlov, E. Shalyt, P. Bratin, and D. M. Tench, in *Copper Interconnects, New Contact Metallurgies/Structures, and Low-k Interlevel Dielectrics II*, G. S. Mathad, V. Bakshi, H. S. Rathore, K. Kondo, and C. Reidsema-Simpson, Editors, PV 2003-10, p. 53, The Electrochemical Society Proceedings Series, Pennington, NJ (2003).
14. W. O. Freitag, C. Ogden, D. Tench, and J. White, *Plat. Surf. Finish.*, **70**, 55 (1983); R. Haak, C. Ogden, and D. Tench, *Plat. Surf. Finish.*, **68**, 52 (1981); R. Haak, C. Ogden, and D. Tench, *Plat. Surf. Finish.*, **69**, 62 (1982).
15. C. Gabrielli, P. Mocoteguy, H. Perrot, D. Nieto-Sanz, and A. Zdunek, *J. Appl. Electrochem.*, **38**, 457 (2008).
16. L. T. Koh, G. Z. You, C. Y. Li, and P. D. Foo, *Microelectron. J.*, **33**, 229 (2002).
17. L. D'Urzo, H. H. Wang, A. Pa, and C. Zhi, *J. Electrochem. Soc.*, **152**, C243 (2005).
18. R. Palmans, S. Claes, L. E. Vanatta, and D. E. Coleman, *J. Chromatogr. A*, **1085**, 147 (2005).
19. M. West, R. McDonald, M. Anderson, S. Kingston, and R. Mui, in *Characterization and Metrology for ULSI Technology 2003*, American Institute of Physics, Melville, NY (2003).
20. T. H. Bailey, Q. Wang, and M. West, *ECS Trans.*, **2**(6), 131 (2007).
21. C.-C. Hung, W-.H. Lee, S.-Y. Hu, S.-C. Chang, K.-W. Chen, and Y-.L. Wang, *J. Electrochem. Soc.*, **155**, H329 (2008).
22. W-.H. Lee, C.-C. Hung, S-.C. Chang, and Y.-L. Wang, *J. Electrochem. Soc.*, **157**, H131 (2010).
23. G. Brisard, N. Bertrand, P. N. Ross, and N. M. Markovic, *J. Electroanal. Chem.*, **480**, 219 (2000).